Appl Nanosci (2014) 4:711–718
DOI 10.1007/s13204-013-0252-7

ORIGINAL ARTICLE

Zirconium(IV) tungstate nanoparticles prepared through chemical co-precipitation method and its function as solid acid catalyst

Manoj Sadanandan · Beena Bhaskaran

Received: 21 April 2013 / Accepted: 22 June 2013 / Published online: 6 July 2013

Abstract In this paper, we report the synthesis of zirconium(IV) tungstate nanoparticles, a new and efficient catalyst for the oxidation of benzyl alcohol and esterification of acetic acid with various alcohols. The nanoparticle catalyst was prepared using the room temperature chemical co-precipitation method. The catalyst was characterized with thermogravimetric and differential thermal analysis, elemental analysis, X-ray diffraction analysis (XRD), fourier transform infrared spectroscopy (FT-IR), high-resolution transmission electron microscopy (HRTEM), atomic force microscopy (AFM) and the Brunauer–Emmett–Teller (BET) surface area. The crystallite size was found to be ~20 nm as revealed by XRD, HRTEM and AFM. The Na^+ exchange capacity was found to be 2.76 meq g^{-1} and the surface area of the compound measured using BET method was found to be 250–265 m^2 g^{-1}. The high value of ion exchange capacity indicates the presence of surface hydroxyl groups. The prepared nanoparticles have proven to be excellent catalysts for both oxidation and ester synthesis under mild reaction conditions. The mechanism of the catalytic reaction was studied as well.

Keywords TMA salt · Zirconium(IV) tungstate · Ion exchange capacity · Catalyst · Oxidation · Esterification

M. Sadanandan (✉) · B. Bhaskaran
Department of Chemistry, Devaswom Board College, Sasthamcotta, Kollam 690521, Kerala, India
e-mail: manojthalavoor@gmail.com

B. Bhaskaran
e-mail: beenadbc@gmail.com

Introduction

Over the past few decades, researchers all over the world were interested in the studies of nanomaterials and their applications have been increasing because of their very different properties at the nanoscale level as compared with those at the macro level. The nanomaterials with high aspect-ratio structures and large surface areas offer exciting research possibilities because of novel physical or chemical properties. Nanomaterials exhibit severalfold enhanced properties such as magnetic, electrical, optical, surface, chemical, catalytic and biological activities due to which these materials show their potential applications in various interdisciplinary areas including biological diagnosis, biomedicine, controlled drug delivery, enzyme immobilization and biosensing. The physical laws applicable to the materials change as the size of the particles decreases to the nanoregime. Surface and quantum effects result in the modification of the properties of nanoparticles (Ali et al. 2009; Ganguli et al. 2008; Si et al. 2007; Hsieh et al. 2010; Gokdai et al. 2010). The recent emergence of nanocatalysis has received a lot of attention because it opens new perspectives for the mild catalysis of important reactions with lower environmental impact.

In view of environmental and economic reasons, the development of nonhazardous chemical processes is a challenge to organic chemists. The use of solid acid catalysts under heterogeneous conditions is one such approach. The various heterogeneous solid acids include metal oxides, zeolites, various microporous and mesoporous materials, clays and clay-based materials, heteropoly acids, ion exchange resins, etc. (Reddy et al. 2005; Guodong et al. 2009; Liao et al. 2011; Yang et al. 2010). The replacement of conventional catalysts with newer solid acid catalysts offer the advantages of non-toxicity, non-corrosiveness, ease of handling and easiness to recover and reuse.

Esterification is an industrially important organic reaction and is used for the synthesis of drug intermediates, additives, dyestuffs, fine chemical intermediates, fragrant chemicals, leather, photographic films, etc. (Hosseini Sarvari and Sharghai 2005; Rabindran Jermy and Pandurajan 2005). Conventional catalysts used for esterification include H_2SO_4, HCl, HF, H_3PO_4, $ClSO_2OH$, etc. These acids are corrosive and the excess acid has to be neutralized after the reaction leaving considerable amount of salts to be disposed off into the environment (Dash and Parida 2007; Palani and Pandurangan 2005; Koster et al. 2001; Liu et al. 2006). Esterification using heterogeneous solid acid catalysts such as ion exchangers avoids the above problems and is therefore gaining importance.

Oxidative catalytic conversion of organic compounds like benzyl alcohol with environmentally clean oxidants such as molecular oxygen or hydrogen peroxide has increased attention because they produce only water as a byproduct. These oxidations require an efficient catalyst (Jamwal et al. 2011; Mardur and Gokavi 2010). Oxidation of benzyl alcohol using supported palladium, heteropoly-acid and Ni–Al-hydrotalcite catalysts with molecular oxygen or aqueous H_2O_2 as the oxidant has been reported (Choudhary et al. 2004). Selective oxidation of benzyl alcohol has also been achieved with H_2O_2 using catalysts such as enzyme laccase (Potthast et al. 1996), hetero polytungstate (Weng et al. 2007), tetra-alkyl pyridinium octamolybdate, Au/U_3O_8, Fe(Cu)-containing coordination polymers, hydrotalcite and layered double hydroxides (Jia et al. 2009).

Tetravalent metal acid (TMA) salts are compounds possessing structural hydroxyl groups. These compounds have the general formula $M^{IV}(HXO_4)_2{\cdot}nH_2O$, where M^{IV} = Zr, Ti, Sn, Th, Ce, etc. and X = W, P, Mo, As, etc. The protons of −OH group in these materials can be exchanged by several cations (Abd El-Latif and Elkady 2011). The presence of replaceable H^+ ions of the −OH groups makes these materials good Bronsted acid catalysts. These materials have been widely studied as catalysts in the amorphous and crystalline forms (Jignasa et al. 2006; Sumej and Raveendran 2008; Patel et al. 2005; Roy et al. 2002). The synthesis of these materials in the nanoform can influence the properties as a whole. The solution phase methods have been considered as one of the most promising routes for the synthesis of nanoparticles owing to less complicated technique, low cost and large-scale production (Li et al. 2009). In the present study, we report the synthesis of zirconium(IV) tungstate nanoparticles and its function as catalysts in oxidation and esterification reactions.

Materials and methods

Synthesis of zirconium(IV) tungstate ion exchanger nanoparticles

The starting materials used for the synthesis of zirconium(IV) tungstate were zirconium(IV) oxychloride, sodium tungstate and ethylene diamine tetra acetic acid (EDTA) disodium salt. All the reagents used were of Analar grade. Nanoparticles of zirconium(IV) tungstate ion exchanger were synthesized by chemical co-precipitation method. For this, in a 250-mL conical flask 25 mL 0.02 M EDTA was taken and 25 mL of 0.2 M zirconium(IV) oxy chloride solution was added from a burette with constant stirring using a magnetic stirrer to obtain homogeneous metal salt solution. To this, 50 mL of 0.2 M sodium tungstate was added drop by drop very slowly from a burette. After the addition of sodium tungstate, the pH of the solution was adjusted to 1–2 by adding 0.1 M HCl. The resulting reaction mixture was then stirred for 2 h. The gel obtained was separated, washed with distilled water and dried. It was then thoroughly ground using an agate mortar and the powder was then converted to the hydrogen form by immersing in 1 M HCl. The acid treated samples were used for further studies.

The chemical stability of the material in various media—acids (HCl, H_2SO_4, HNO_3, HF and aquaregia), bases (NaOH and KOH) and organic solvents (ethanol, benzene, acetone and acetic acid) was studied by taking 100 mg each of synthesized material in 50 mL of the particular media and allowing to stand for 24 h. The changes in colour, nature and weight were observed.

Determination of ion exchange capacity (i.e.c)

In the present study, the ion exchange capacity (i.e.c) of the ion exchanger nanoparticles was determined by column method. The column was prepared in a burette, provided with glass wool at the bottom. It was filled half way with distilled water, preventing air traps and then 0.5 g of the ion exchanger nanoparticles was accurately weighed and transferred through a dry funnel. The water inside the column was kept at a level of about 1 cm above the material. In order to determine the Na^+ exchange capacity, 250 mL solution of sodium acetate was added into the column and elution was carried out at a flow rate of 0.5 mL min^{-1}. The eluant was collected in a 500-mL conical flask and then titrated against 0.1 N NaOH solution. The i.e.c of the exchanger in milliequivalent per gramme (meq g^{-1}) is given by the following relation:

$$\text{i.e.c} = \frac{av}{w},$$

where a is the molarity of the NaOH solution, v is the volume of the NaOH required for titration and w is the weight of the exchanger. The i.e.c were also determined for other alkali metals like Li^+ and K^+ and alkaline earth metal ions like Mg^{2+}, Ca^{2+}, Sr^{2+} and Ba^{2+} using the same method. The effect of heat on the ion exchange capacity of the material was also studied by heating 1 g portions of the exchanger for 2 h each at various temperatures from 100 to 700 °C in a muffle furnace and then determining the i.e.c as usual by the column method.

Characterization techniques

To determine whether there is any phase transition, thermogravimetric and differential thermal analysis (TGA/DTA) of the as prepared ion exchanger nanoparticles was recorded on a Shimadzu Thermal Analyzer at a heating rate of 10 °C min^{-1} in air atmosphere. It allows obtaining simultaneous TGA and DTA under the same condition. The chemical composition of the ion exchanger nanoparticles were analysed using elemental analysis (EDS), taken using JOEL Model JED-2300. The material was characterized by powder X-ray diffraction (XRD) using X-ray diffractometer (Model XPERT-PRO) with nickel filtered Cu–Kα radiation (λ = 1.5406 Å). The infrared spectrum of the sample was taken in the region between 4,000 and 400 cm^{-1} on a Thermo-Nicolet Avatar 370 model Fourier Transform infrared spectrometer using KBr pellet. For this samples were prepared by mixing with KBr and then made into pellet. The particle size and morphology of the co-precipitated powders were observed by HRTEM taken using 300 kV HRTEM (FEI-model) Tecnai 30 G2 instrument and AFM taken using NTEGRA (NT MDT) NSG 10 model AFM instrument by contact mode. Surface area measurement (BET method) was carried out on Micromeritrics Gemini at −195 °C using nitrogen atmosphere.

Esterification

The esterification of acetic acid with various alcohols (Scheme 1) were carried out in a round-bottomed flask (100 cm^3) fitted with a water-cooled condenser. The temperature was maintained at 110 °C using an oil bath connected to a thermostat. In a typical reaction, acetic acid and alcohol were taken in the ratio of 2:1 directly into the round-bottomed flask along with the ion exchanger nanoparticle catalyst. To this reaction mixture, 10−15 mL of a suitable solvent such as toluene or cyclohexane was added. Cyclohexane was used as the solvent for synthesis of ethyl acetate and toluene for other acetates. Reaction mixture was refluxed for 2.5 h. Products were analysed using GC–MS. The reaction conditions were optimized after changing the reaction conditions like ratio of acid to alcohol, amount of catalyst and solvent.

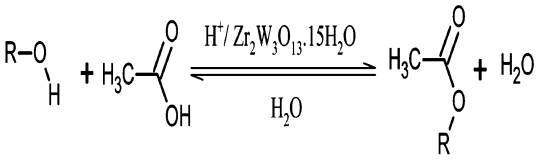

Scheme 1 Esterification of acetic acid with various alcohols

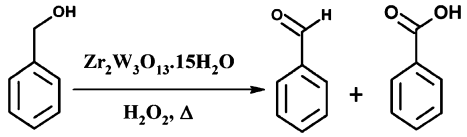

Scheme 2 Oxidation of benzyl alcohol

Oxidation

Oxidation of benzyl alcohol (Scheme 2) was carried out in a 100-mL round-bottomed flask equipped with water condenser. First, a mixture of benzyl alcohol and hydrogen peroxide was taken in 2:1 volume ratio and 1 mL acetonitrile was added as solvent. To this 100 mg of nanoparticles of zirconium(IV) tungstate ion exchanger was added and refluxed for two and half hours at two different temperatures, i.e. 85 and 110 °C. The reactions were also carried out in the absence of acetonitrile and catalyst. The products were analysed using GC–MS.

Results and discussion

Ion exchange capacity

Zircoinum(IV) tungstate ion exchanger was obtained as a white powder. The material was found to be stable in mineral acids and bases at all concentrations as evidenced by no change in colour, form or weight of the sample used

Table 1 Ion exchange capacities of Zirconium(IV) tungstate nanoparticles using respective metal chlorides

Ion exchanged	Ionic radius (Å)	Hydrated ionic radius (Å)	Ion exchange capacity (meq g^{-1})
Li^+	0.68	3.40	1.48
Na^+	0.97	2.76	1.98
K^+	1.33	2.32	2.30
Mg^{2+}	0.78	7.00	1.40
Ca^{2+}	1.06	6.30	1.63
Sr^{2+}	1.27	6.10	1.84
Ba^{2+}	1.43	5.90	2.50

Table 2 Effect of heat on the Na^+ exchange capacities for Zirconium(IV) tungstate nanoparticles

Sample at	RT	100 °C	300 °C	500 °C	700 °C
Colour/appearance	White	Dirty white	Grey	Yellowish white	Greenish Yellow
i.e.c	1.98	1.60	0.80	0.20	0.20

RT *Room temperature*

except in HF and aquaregia. The exchanger was also stable in alkali and alkaline earth metal ions. The ion exchange capacities for different alkali and alkaline earth metal ions are shown in Table 1. It is clear from the table that the i.e.c increases with decreasing hydrated ionic radii for mono and bivalent metal ions. This shows that ion exchange takes place in the hydrated ionic form. The Na^+ exchange capacity for amorphous zirconium(IV) tungstate was reported to be 1.32 meq g^{-1} (Parikh and Chudasama 2003). The large value of i.e.c for this material is due to the nano-sized nature and hence the large surface area of these materials. The effect of heat on Na^+ ion exchange capacity is shown in Table 2. The ion exchange capacity decreases with increase in annealing temperature due to the condensation of structural hydroxyl groups. The high-value of ion exchange capacity indicates the presence of large number of surface hydroxyl groups and hence the high Bronsted acidity.

TGA, DTA and EDS analysis

Thermogram of the ion exchanger nanoparticles shows 20.21 % weight loss in the region ~100 °C due to the loss of moisture or hydrated water molecules. A gradual weight loss was observed after 100 °C due to the condensation of structural hydroxyl groups. Above 100 °C, condensation of structural hydroxyl groups takes place which is characteristic of synthetic inorganic ion exchangers. The DTA curve also supports this behaviour. The decrease in the value of i.e.c with annealing temperatures is also a supporting evidence for the loss of hydroxyl groups at higher temperature. The energy dispersive spectrum of this exchanger is shown in Fig. 1. The percentage composition thus obtained was found to be 20.50 % zirconium, 57.34 % tungsten and 22.61 % oxygen. The mole ratio of Zr:W was found to be 2:3 suggesting an empirical formula of $Zr_2W_3O_{13}{\cdot}nH_2O$, where '*n*' is the number of water molecules. The value of '*n*', the number of external water molecules was calculated using Alberti equation (Alberti et al. 1966). The number of water molecules calculated for the ion exchanger using this equation was found to be 15. The formula thus assigned to the compound is $Zr_2W_3O_{13}{\cdot}15H_2O$.

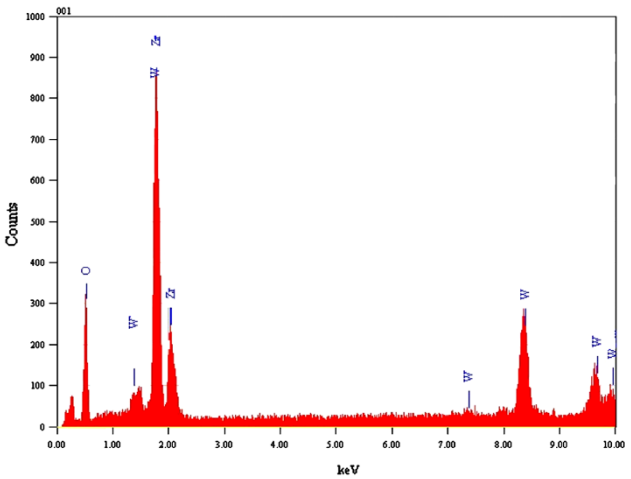

Fig. 1 EDS of zirconium(IV) tungstate ion exchanger nanoparticles

XRD analysis

Figure 2a shows the XRD pattern of the as prepared powder obtained by the co-precipitation method. All of the peaks in the spectrum well matched with that of bulk cubic ZrW_2O_8 (JCPDS Card No.89-6670), with small amount of cubic zirconia (JCPDS file No.89-9069) and hexagonal tungsten oxide (JCPDS file No.82-2459). No other peaks related to impurities were detected in the spectrum, which further confirms the phase purity of the synthesized powder. Statistical analysis of the particle size distribution of the ion exchanger nanoparticle shows that the mean size is around 20 nm which is in consistent with the particle size obtained from XRD pattern. The crystallite size estimated from X-ray line broadening using Scherrer equation was ~19 nm. The particle size distribution curve shows distribution of particles ranging from 10 to 28 nm and centred at ~19 nm as shown in the particle size histogram of Fig. 2b.

FT-IR analysis

The FT-IR spectrum of the ion exchanger taken at room temperature is shown in Fig. 3. It gives idea about different bonding mode in this material. The presence of water molecules was identified from the bands observed in the region ~3,415, ~1,637 and ~1,380 cm^{-1}. Band in the region ~837 cm^{-1} was due to WO_4^{2-} species and

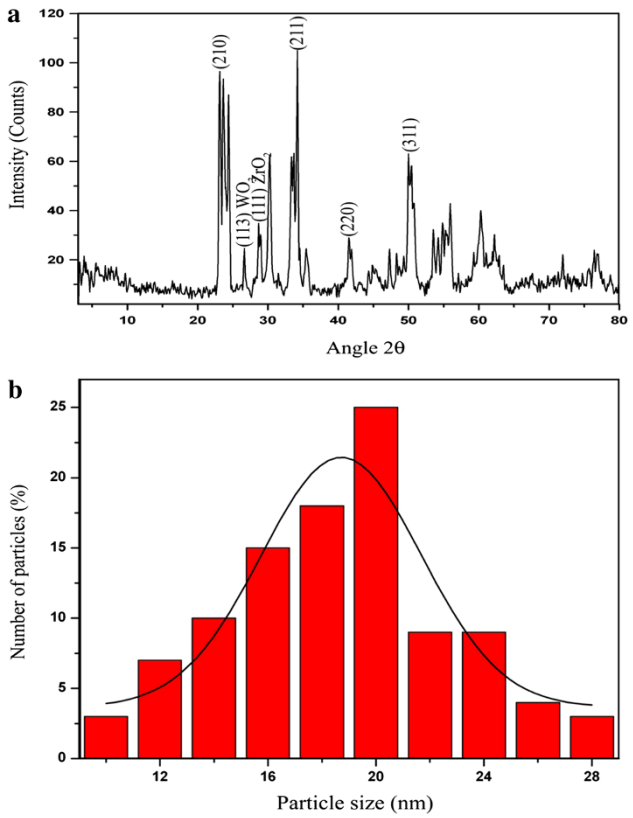

Fig. 2 **a** XRD pattern of as prepared zirconium(IV) tungstate ion exchanger nanoparticles. **b** Particle size histogram of zirconium(IV) tungstate ion exchanger nanoparticles

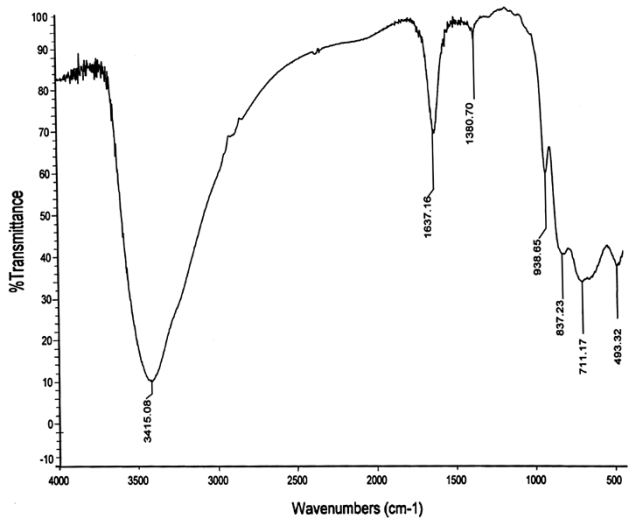

Fig. 3 FT-IR spectra of zirconium(IV) tungstate ion exchanger nanoparticles

at $\sim$711 cm^{-1} was due to W–O stretching vibration. Band in the region $\sim$493 cm^{-1} corresponds to Zr–O vibration (Rao et al. 2006; Liu et al. 2006). The FT-IR spectrum also shows the phase pure nature of the compound.

HRTEM, AFM and surface area analysis

The particle size of the powders can be determined from the HRTEM picture. The HRTEM method is better than X-ray line broadening, as it is direct and less affected by experimental errors and/or other properties of the particles such as internal strain or distribution in the size of the lattice parameter. Figure 4 is the HRTEM micrograph of the powder synthesized through room temperature co-precipitation method. The average grain size observed from the micrograph is about 20–35 nm, which is in agreement with the calculation using Scherrer equation. The morphology of the $Zr_2W_3O_{13}\cdot 15H_2O$ nanoparticles analysed by AFM (Fig. 5) shows the formation of nanoparticles with

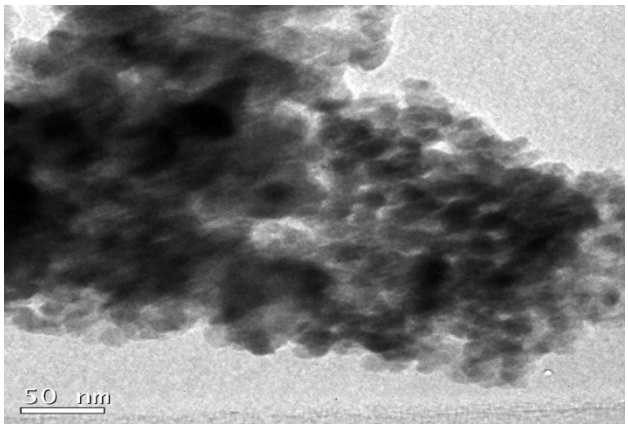

Fig. 4 HRTEM bright field image of zirconium(IV) tungstate ion exchanger nanoparticles

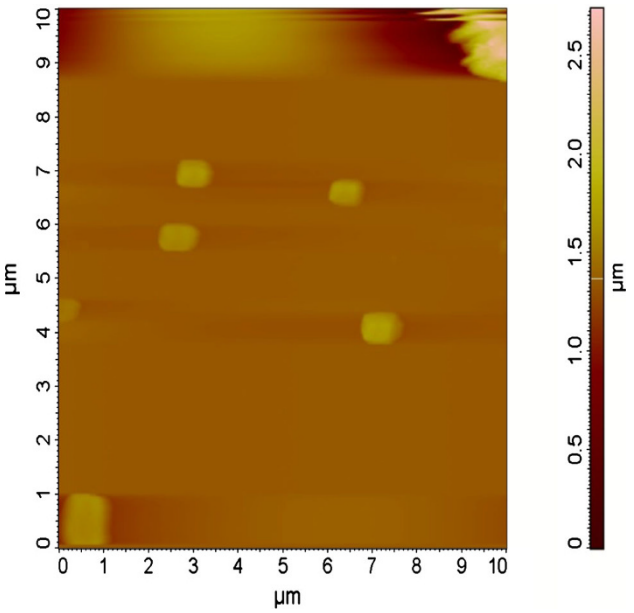

Fig. 5 AFM image of zirconium(IV) tungstate ion exchanger nanoparticles

sizes in the range 15–35 nm with an average of ~20 nm diameter. The surface area of the ion exchanger nanoparticles measured by using BET method was found to be 250–265 $m^2\ g^{-1}$.

Esterification

Esterification reaction is relatively slow and needs activation either by high temperature or by a catalyst to achieve equilibrium conversion to a reasonable amount. Esterification is reversible and equilibrium constants for these reactions are low. One of the products during esterification is water. In order to obtain higher yield of esters, the reaction must be forced to completion by either removing the water produced or by operating with an excess of one of the two reactants, acid or alcohol. In the present work acid was taken in excess. The presence of water formed during the esterification could result in the occurring of hydrolysis reaction, which also reduces the production yield. The effect of adding a co-solvent increases the rate of reaction and production yield. Therefore, solvents such as cyclohexane and toluene were employed in the present reaction to remove the water formed during the reaction as a binary azeotrope so that reverse reaction is avoided (Mongkkolbovornkij et al. 2010; Joshi et al. 2008).

The reaction conditions were first optimized for methyl acetate. The condition that gave maximum yield of ester was selected and the same conditions were used for the synthesis of other esters. The optimum condition that gave maximum yield of methyl acetate was as follows: amount of catalyst—100 mg, reaction time—2.5 h and acid to alcohol mole ratio—2:1. Table 3 shows the percentage yields of various esters obtained in the present study. In the case of isomeric alcohols, the yield decreases in the order $1^\circ > 2^\circ > 3^\circ$. The lower yield of tertiary alcohols is due to steric interaction (Chen et al. 2008). In the case of regenerated sample, the yield decreases by 5 % only after five cycles. The yield becomes constant on further regeneration. Among the esters prepared using this catalyst, higher yield

Table 3 Percentage yield of different esters

Case	Esters formed	% Conversion
1	Methyl acetate	78
2	Ethyl acetate	82
3	Propyl acetate	75
4	Isopropyl acetate	60
5	Butyl acetate	78
6	2°-Butyl acetate	64
7	3°-Butyl acetate	57
8	Amyl acetate	84
9	Benzyl acetate	85

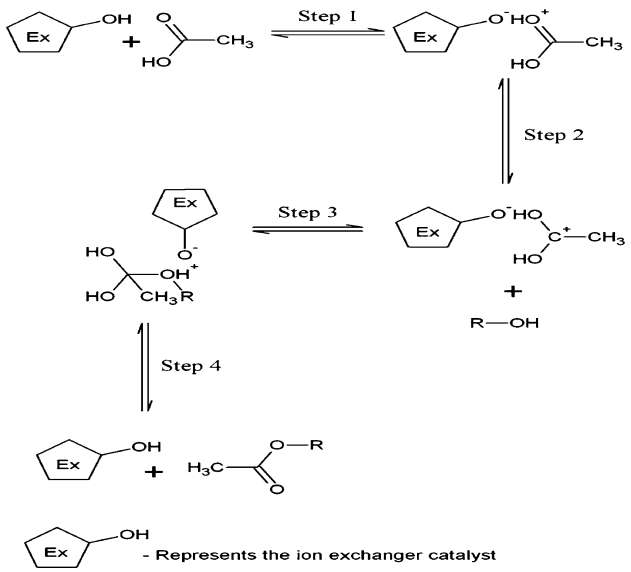

Fig. 6 Probable mechanism of esterification of acetic acid

is obtained in the case of benzyl acetate which could be attributed to the enhanced nucleophilicity due to the presence of aromatic ring in benzyl alcohol. Literature shows that for micrometer-sized similar bulk catalysts, the amount of catalyst required is more with a higher refluxing time (Joshi et al. 2008; Ma et al. 1996; Bhatt and Patel 2005). But in the present case only 100 mg of catalyst was used and the refluxing time was only 2.5 h. The catalytic activity of the $Zr_2W_3O_{13}{\cdot}15H_2O$ nanoparticles was initiated by the adsorption of acid on the catalyst resulting in the formation of a carbocation intermediate followed by the attack of alcohol resulting in the formation of ester with the regeneration of the catalyst. The possible mechanism for the esterification is given in scheme as shown in Fig. 6. It shows that the catalyst with Bronsted acid sites help in the formation of carbocation intermediate. In conventional method, H_2SO_4 is used as catalyst for preparing esters, the yield is high but it is difficult to remove traces of H_2SO_4 present. The isolation of products requires aqueous quenching and neutralization. The water eliminated during the conversion dilutes the acid, weakening the acid catalyst and hence great quantity of acid is required. The uses of solid acid catalyst like nano zirconium tungstate are advantageous, since there is no catalyst contamination and the ester can be simply distilled off.

Oxidation

Oxidation of benzyl alcohol gives benzaldehyde, benzoic acid and benzyl benzoate. It gives series reactions: in the first step benzyl alcohol oxidizes into benzaldehyde and in the next step benzaldehyde gets oxidized to benzoic acid.

Table 4 Results of oxidation of benzyl alcohol (BA), conversion and selectivity

Case	BA:H_2O_2 and temp (°C)	CN (mL)	% Yield	Selectivity (%)	
				−CHO	−COOH
1	1:1, 110	1	71.80	79.96	20.04
2	1:1, 110	–	73.20	72.60	27.39
3	1:1, 82	1	65.38	81.90	18.10
4	1:1, 82	–	70.50	81.39	18.60
5[a]	1:1, 82	1	20.00	84.34	15.65
6[a]	1:1, 82	–	15.00	77.70	22.29

[a] Reactions were carried out in the absence of catalyst

In the present case, only benzaldehyde and benzoic acid were obtained as products. The percentage yield was found to be high using a small quantity of the nano zirconium tungstate catalyst (100 mg). The reactions were carried out at two different temperatures with and without a solvent. This reaction slowly proceeded in the absence of the catalyst. A similar observation was also noted by other authors (Huang et al. 2006). As shown in Table 4, the percentage yield was found to be very low in the absence of the catalyst. However, on using the $Zr_2W_3O_{13}{\cdot}15H_2O$ nanoparticles as catalysts the yield was found to be very much increased. The selectivity was found to be high for benzaldehyde on using this catalyst. It was also noticed that increase in temperature increases selectivity towards benzoic acid.

The exchanger contains WO_x discrete clusters with tungsten in +6 oxidation state. Bronsted acid sites were formed from these clusters when Zr^{4+} replaces W^{6+} from their sites or when W^{6+} centres reduces slightly during catalytic reaction (Barton et al. 1998). The catalyst contains W=O oxospecies on the discrete clusters which converts to W-OH species in the presence of water or moisture. The −OH groups on the surface of the catalyst combine with H_2O_2 to form metal peroxo compound and transfer peroxidic oxygen to the reactant (Venkatathri 2004). A suitable mechanism has been proposed for the reaction as given in scheme shown in Figs. 7 and 8. In this type of catalysts, Bronsted acid sites (acidity) were also formed on the surface of the catalysts in situ by partial reduction during catalytic reactions (Satsuma 2007).

Catalysis based on nanocatalysts is a very promising method in industrial applications. We could distinguish two different applications of the synthesized $Zr_2W_3O_{13}{\cdot}15H_2O$ nanoparticles as catalysts: in esterification and in oxidation. Both these reactions play an important role in the field of synthesis of various organic compounds of industrial use and functional group transformations. The catalyst can be easily separated by simple filtration and regenerated and reused, thus making the process economical and environmentally benign.

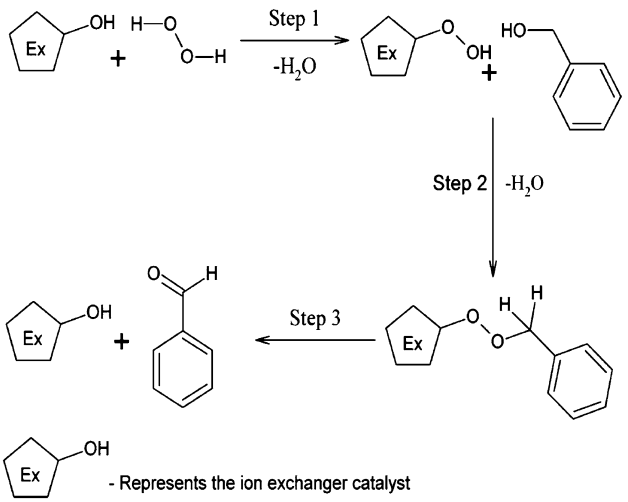

Fig. 7 Probable mechanism of oxidation of benzyl alcohol into benzaldehyde

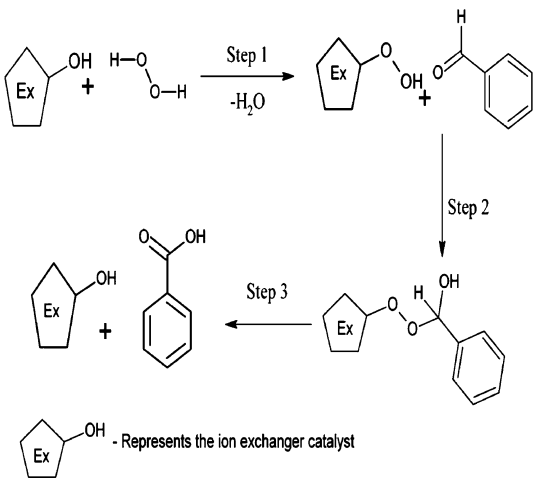

Fig. 8 Probable mechanism of the oxidation of benzaldehyde into benzoic acid

Conclusion

In conclusion, we have demonstrated the catalytic activity of $Zr_2W_3O_{13}{\cdot}15H_2O$ nanoparticles. The catalyst

$Zr_2W_3O_{13}{\cdot}15H_2O$ was synthesized by chemical co-precipitation method. XRD results showed that it consists of pure phase with very good crystallinity. The particle size obtained from Scherrer formula was in good agreement with HRTEM and AFM results. The $Zr_2W_3O_{13}{\cdot}15H_2O$ catalyst possesses the virtue of high catalytic efficiency, relatively good selectivity, simple preparation, easy recovery and being friendly to equipment and environment. The catalyst is highly active for the esterification of acetic acid with different alcohols. The $Zr_2W_3O_{13}{\cdot}15H_2O$ is a stable, economic and high active catalyst for oxidation of benzyl alcohol using H_2O_2 as oxidant at reflux condition. The improvement of catalytic activity was attributed to the increase of surface area and the increased number of Bronsted acid sites. The catalytic performances of the re-used $Zr_2W_3O_{13}{\cdot}15H_2O$ catalysts, even for using five times, were comparable with that of the fresh catalyst, giving this catalyst a good prospect in industry.

Acknowledgments The authors are thankful to the Principal, D.B. College, Sasthamcotta, for providing the necessary laboratory facilities and to Dr. A. Ajayaghosh, NIIST, Thiruvananthapuram for AFM facilities. M.S is thankful to the UGC, New Delhi, for financial assistance.

References

Abd El-Latif MM, Elkady MF (2011) Desalination 271:41
Alberti G, Torraca E, Conte G (1966) J Inorg Nucl Chem 28:607
Ali SR, Bansal VK, Khan AA, Jain SK, Ansari MA (2009) J Mol Catal A: Chem 303:60
Barton DG, Soled SL, Iglesia Enrique (1998) Top Catal 6:87
Bhatt N, Patel A (2005) J Mol Catal A 238:223
Chen Shuan-Hu, Zhao Q, Xue-Wang X (2008) J Chem Sci 120:481
Choudhary VR, Dumbre DK, Uphade BS, Narkhede VS (2004) J Mol Catal A Chem 215:129
Dash SS, Parida KM (2007) J Mol Catal A: Chem 266:88
Ganguli AK, Vaidya Sonalika, Ahmed Tokeer (2008) Bull Mater Sci 31:415
Gokdai Z, Sınag A, Yumak T (2010) Biomass Bioenergy 34:402
Guodong F, Mao S, Zhao Z, Farui J (2009) J Rare Earths 27:437
Hosseini Sarvari M, Sharghai H (2005) Tetrahedron 61:10903
Hsieh Y-T, Huang M-W, Chang C-C, Chen U-S, Shih H-C (2010) Thin Solid Films 519:1668
Huang JY, Li SJ, Wang YG (2006) Tetrahedron Lett 47:5637
Jamwal Navjot, Sodhi RK, Gupta P, Paul S (2011) Int J Biol Macromol 49:930
Jia A, Lou L–L, Zhang C, Zhang Y, Liu S (2009) J Mol Catal A: Chem 306:123
Jignasa A, Rajesh T, Uma C (2006) J Chem Sci 118:185
Joshi R, Patel H, Chudasama U (2008) Ind J Chem Techn 15:238
Koster R, van der Linden B, Poels E, Bliek A (2001) J Catal 204:333
Li Y-F, Jia-Hu Ouyang Yu, Zhou X-SL, Zhong J-Y (2009) Bull Mater Sci 32:149
Liao Y, Huang X, Liao X, Shi B (2011) J Mol Catal A: Chem 347:146
Liu Y, Lotero E, Goodwin JG (2006a) J Catal 242:278
Liu Xuanyong, Huang Anping, Ding Chuanxian, Chu PaulK (2006b) Biomaterials 27:3904
Ma Y, Wang QL, Yan H, Ji X, Qui Q (1996) Appl Catal A Gen 139:362–367
Mardur SP, Gokavi GS (2010) J Iran Chem Soc 7:441–446
Mongkkolbovornkij P, Champreda V, Sutthisripok W, Laosiripojana V (2010) Fuel Proc Tech 91:1510
Palani A, Pandurangan A (2005) J Mol Catal A Chem 226:129
Parikh A, Chudasama U (2003) Proc Ind Acad Sci (Chem Sci) 115:15
Patel H, Parikh A, Chudasama U (2005) Bull Mater Sci 28:137
Potthast A, Rosenau T, Chen CL, Gratzl JS (1996) J Mol Catal A Chem 10:5
Rabindran Jermy B, Pandurajan A (2005) J Mol Catal A 237:146
Rao KN, Sridhar A, Lee AF, Taveneer SJ, Yong NA, Wilson K (2006) Green Chem 8:790
Reddy BM, Sreekanth PM, Vangala R (2005) J Mol Catal A 225:71
Roy K, Pal DK, Basu S, Nayaka D, Lahiri S (2002) Appl Rad Isot 57:471
Satsuma A, Shimizu K, Shiwagi KK, Endo T, Nishiyama H, Kakimoto S, Sugaya S, Yokoi H (2007) J Phys Chem C 111:12080–12085
Si PZ, Choi CJ, Bruck E, Klaasse JCP, Geng DY, Zhang ZD (2007) Physica B 392:154
Sumej C, Raveendran B (2008) Bull Mater Sci 31:613
Venkatathri N (2004) Indian J Chem. 43A:2315
Weng ZH, Wang JY, Jian XG (2007) Chin Chem Lett 18:936
Yang Z, Zhoua C, Zhang W, Li H, Chena M (2010) Colloids Surf A: Physicochem Eng Aspects 356:134